

# ***Microwave Devices and Circuits***

***Third Edition***

**SAMUEL Y. LIAO**

*Professor of Electrical Engineering  
California State University, Fresno*

Prentice-Hall



**PRENTICE HALL, Englewood Cliffs, New Jersey 07632**

## Chapter 7

# Transferred Electron Devices (TEDs)

### **7-0 INTRODUCTION**

The application of two-terminal semiconductor devices at microwave frequencies has been increased usage during the past decades. The CW, average, and peak power outputs of these devices at higher microwave frequencies are much larger than those obtainable with the best power transistor. The common characteristic of all active two-terminal solid-state devices is their negative resistance. The real part of their impedance is negative over a range of frequencies. In a positive resistance the current through the resistance and the voltage across it are in phase. The voltage drop across a positive resistance is positive and a power of ( $I^2 R$ ) is dissipated in the resistance. In a negative resistance, however, the current and voltage are out of phase by  $180^\circ$ . The voltage drop across a negative resistance is negative, and a power of ( $-I^2 R$ ) is generated by the power supply associated with the negative resistance. In other words, positive resistances absorb power (passive devices), whereas negative resistances generate power (active devices). In this chapter the transferred electron devices (TEDs) are analyzed.

The differences between microwave transistors and transferred electron devices (TEDs) are fundamental. Transistors operate with either junctions or gates, but TEDs are bulk devices having no junctions or gates. The majority of transistors are fabricated from elemental semiconductors, such as silicon or germanium, whereas TEDs are fabricated from compound semiconductors, such as gallium arsenide (GaAs), indium phosphide (InP), or cadmium telluride (CdTe). Transistors operate with “warm” electrons whose energy is not much greater than the thermal energy (0.026 eV at room temperature) of electrons in the semiconductor, whereas TEDs

operate with "hot" electrons whose energy is very much greater than the thermal energy. Because of these fundamental differences, the theory and technology of transistors cannot be applied to TEDs.

## 7-1 GUNN-EFFECT DIODES—*GaAs DIODE*

Gunn-effect diodes are named after J. B. Gunn, who in 1963 discovered a periodic fluctuations of current passing through the *n*-type gallium arsenide (GaAs) specimen when the applied voltage exceeded a certain critical value. Two years later, in 1965, B. C. DeLoach, R. C. Johnston, and B. G. Cohen discovered the impact ionization avalanche transit-time (IMPATT) mechanism in silicon, which employs the avalanching and transit-time properties of the diode to generate microwave frequencies. In later years the limited space-charge-accumulation diode (LSA diode) and the indium phosphide diode (InP diode) were also successfully developed. These are bulk devices in the sense that microwave amplification and oscillation are derived from the bulk negative-resistance property of uniform semiconductors rather than from the junction negative-resistance property between two different semiconductors, as in the tunnel diode.

### 7-1-1 *Background*

After inventing the transistor, Shockley suggested in 1954 that two-terminal negative-resistance devices using semiconductors may have advantages over transistors at high frequencies [1]. In 1961 Ridley and Watkins described a new method for obtaining negative differential mobility in semiconductors [2]. The principle involved is to heat carriers in a light-mass, high-mobility subband with an electric field so that the carriers can transfer to a heavy-mass, low-mobility, higher-energy subband when they have a high enough temperature. Ridley and Watkins also mentioned that Ge–Si alloys and some III–V compounds may have suitable subband structures in the conduction bands. Their theory for achieving negative differential mobility in bulk semiconductors by transferring electrons from high-mobility energy bands to low-mobility energy bands was taken a step further by Hilsum in 1962 [3]. Hilsum carefully calculated the transferred electron effect in several III–V compounds and was the first to use the terms transferred electron amplifiers (TEAs) and oscillators (TEOs). He predicted accurately that a TEA bar of semi-insulating GaAs would be operated at 373°K at a field of 3200 V/cm. Hilsum's attempts to verify his theory experimentally failed because the GaAs diode available to him at that time was not of sufficiently high quality.

It was not until 1963 that J. B. Gunn of IBM discovered the so-called Gunn effect from thin disks of *n*-type GaAs and *n*-type InP specimens while studying the noise properties of semiconductors [4]. Gunn did not connect—and even immediately rejected—his discoveries with the theories of Ridley, Watkins, and Hilsum. In 1963 Ridley predicted [5] that the field domain is continually moving down through the crystal, disappearing at the anode and then reappearing at a favored nucleating

center, and starting the whole cycle once more. Finally, Kroemer stated [6] that the origin of the negative differential mobility is Ridley–Watkins–Hilsum's mechanism of electron transfer into the satellite valleys that occur in the conduction bands of both the *n*-type GaAs and the *n*-type InP and that the properties of the Gunn effect are the current oscillations caused by the periodic nucleation and disappearance of traveling space-charge instability domains. Thus the correlation of theoretical predictions and experimental discoveries completed the theory of transferred electron devices (TEDs).

### 7-1-2 Gunn Effect

A schematic diagram of a uniform *n*-type GaAs diode with ohmic contacts at the end surfaces is shown in Fig. 7-1-1. J. B. Gunn observed the Gunn effect in the *n*-type GaAs bulk diode in 1963, an effect best explained by Gunn himself, who published several papers about his observations [7 to 9]. He stated in his first paper [7] that

Above some critical voltage, corresponding to an electric field of 2000–4000 volts/cm, the current in every specimen became a fluctuating function of time. In the GaAs specimens, this fluctuation took the form of a periodic oscillation superimposed upon the pulse current. . . . The frequency of oscillation was determined mainly by the specimen, and not by the external circuit. . . . The period of oscillation was usually inversely proportional to the specimen length and closely equal to the transit time of electrons between the electrodes, calculated from their estimated velocity of slightly over  $10^7$  cm/s. . . . The peak pulse microwave power delivered by the GaAs specimens to a matched load was measured. Value as high as 0.5 W at 1 Gc/s, and 0.15 W at 3 Gc/s, were found, corresponding to 1–2% of the pulse input power.\*

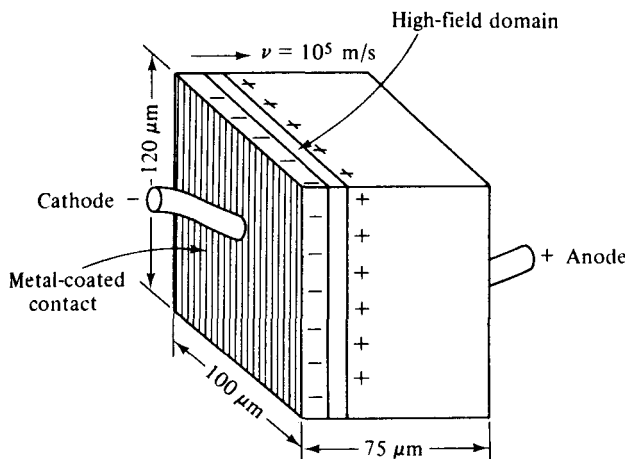


**Figure 7-1-1** Schematic diagram for *n*-type GaAs diode.

\*After J. B. Gunn [7]; reproduced by permission of IBM, Inc.

From Gunn's observation the carrier drift velocity is linearly increased from zero to a maximum when the electric field is varied from zero to a threshold value. When the electric field is beyond the threshold value of 3000 V/cm for the *n*-type GaAs, the drift velocity is decreased and the diode exhibits negative resistance. This situation is shown in Fig. 7-1-2.

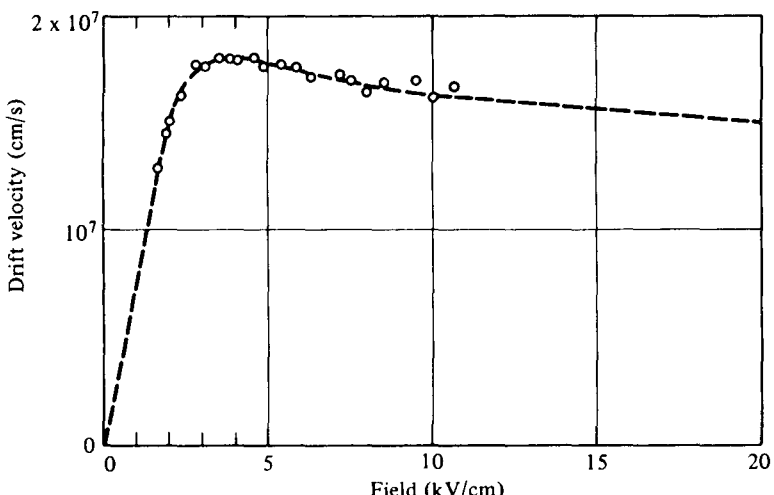


**Figure 7-1-2** Drift velocity of electrons in *n*-type GaAs versus electric field.  
(After J. B. Gunn [8]; reprinted by permission of IBM, Inc.)

The current fluctuations are shown in Fig. 7-1-3. The current waveform was produced by applying a voltage pulse of 16-V amplitude and 10-ns duration to a specimen of *n*-type GaAs  $2.5 \times 10^{-3}$  cm in length. The oscillation frequency was 4.5 GHz. The lower trace had 2 ns/cm in the horizontal axis and 0.23 A/cm in the vertical axis. The upper trace was the expanded view of the lower trace. Gunn found that the period of these oscillations was equal to the transit time of the electrons through the specimen calculated from the threshold current.

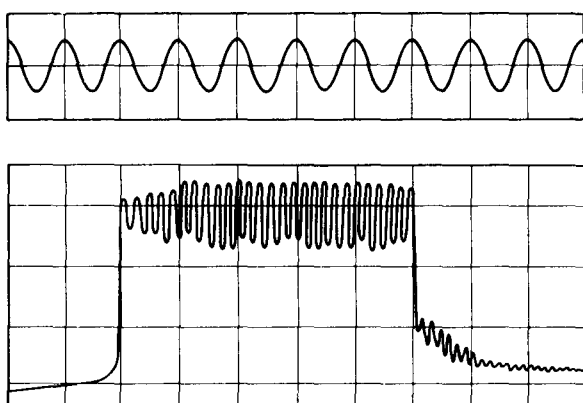


**Figure 7-1-3** Current waveform of *n*-type GaAs reported by Gunn. (After J. B. Gunn [8]; reprinted by permission of IBM, Inc.)

Gunn also discovered that the threshold electric field  $E_{th}$  varied with the length and type of material. He developed an elaborate capacitive probe for plotting the electric field distribution within a specimen of  $n$ -type GaAs of length  $L = 210 \mu\text{m}$  and cross-sectional area  $3.5 \times 10^{-3} \text{ cm}^2$  with a low-field resistance of  $16 \Omega$ . Current instabilities occurred at specimen voltages above 59 V, which means that the threshold field is

$$E_{th} = \frac{V}{L} = \frac{59}{210 \times 10^{-6} \times 10^2} = 2810 \text{ volts/cm} \quad (7-1-1)$$

## 7-2 RIDLEY–WATKINS–HILSUM (RWH) THEORY

Many explanations have been offered for the Gunn effect. In 1964 Kroemer [6] suggested that Gunn's observations were in complete agreement with the Ridley–Watkins–Hilsum (RWH) theory.

### 7-2-1 Differential Negative Resistance

The fundamental concept of the Ridley–Watkins–Hilsum (RWH) theory is the differential negative resistance developed in a bulk solid-state III–V compound when either a voltage (or electric field) or a current is applied to the terminals of the sample. There are two modes of negative-resistance devices: voltage-controlled and current-controlled modes as shown in Fig. 7-2-1(a) and (b), respectively [5].

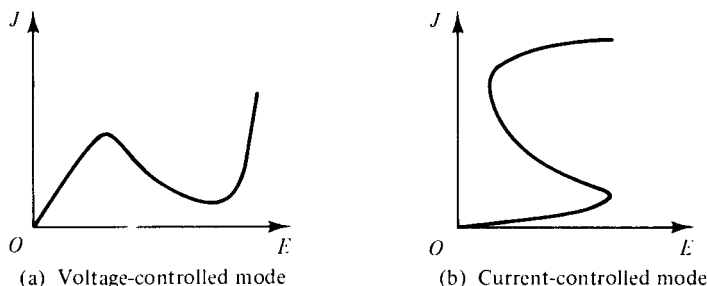


**Figure 7-2-1** Diagram of negative resistance. (From B. K. Ridley [5]; reprinted by permission of the Institute of Physics.)

In the voltage-controlled mode the current density can be multivalued, whereas in the current-controlled mode the voltage can be multivalued. The major effect of the appearance of a differential negative-resistance region in the current-density-field curve is to render the sample electrically unstable. As a result, the initially homogeneous sample becomes electrically heterogeneous in an attempt to reach stability. In the voltage-controlled negative-resistance mode high-field domains are formed, separating two low-field regions. The interfaces separating low- and high-field domains lie along equipotentials; thus they are in planes perpendicular to the current direction as shown in Fig. 7-2-2(a). In the current-controlled negative-resistance mode splitting the sample results in high-current filaments running along the field direction as shown in Fig. 7-2-2(b).

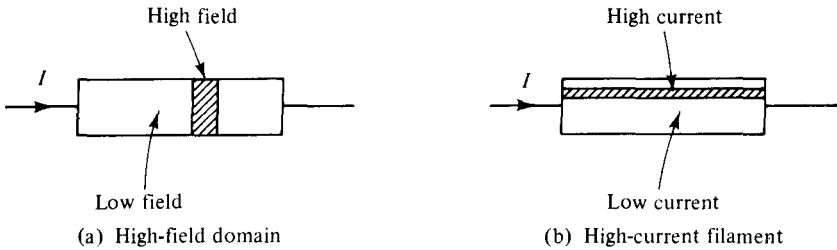


**Figure 7-2-2** Diagrams of high field domain and high current filament. (From B. K. Ridley [5]; reprinted by permission of the Institute of Physics.)

Expressed mathematically, the negative resistance of the sample at a particular region is

$$\frac{dI}{dV} = \frac{dJ}{dE} = \text{negative resistance} \quad (7-2-1)$$

If an electric field  $E_0$  (or voltage  $V_0$ ) is applied to the sample, for example, the current density  $J_0$  is generated. As the applied field (or voltage) is increased to  $E_2$  (or  $V_2$ ), the current density is decreased to  $J_2$ . When the field (or voltage) is decreased to  $E_1$  (or  $V_1$ ), the current density is increased to  $J_1$ . These phenomena of the voltage-controlled negative resistance are shown in Fig. 7-2-3(a). Similarly, for the current-controlled mode, the negative-resistance profile is as shown in Fig. 7-2-3(b).

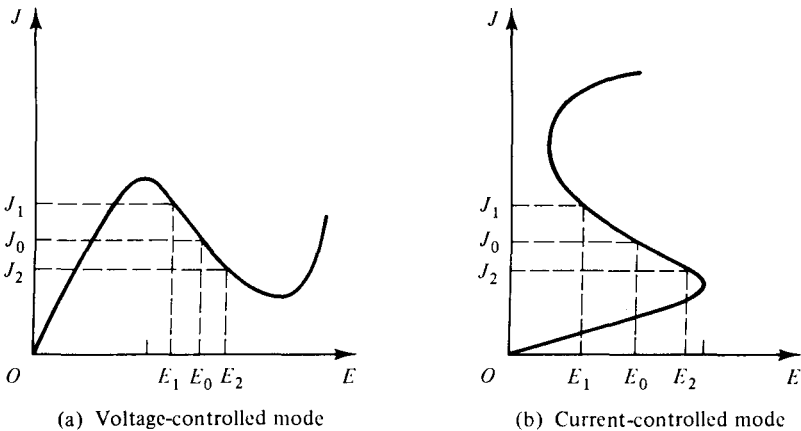


**Figure 7-2-3** Multiple values of current density for negative resistance. (From B. K. Ridley [5]; reprinted by permission of the Institute of Physics.)

### 7-2-2 Two-Valley Model Theory

A few years before the Gunn effect was discovered, Kroemer proposed a negative-mass microwave amplifier in 1958 [10] and 1959 [11]. According to the energy band theory of the  $n$ -type GaAs, a high-mobility lower valley is separated by an energy of 0.36 eV from a low-mobility upper valley as shown in Fig. 7-2-4. Table 7-2-1 lists

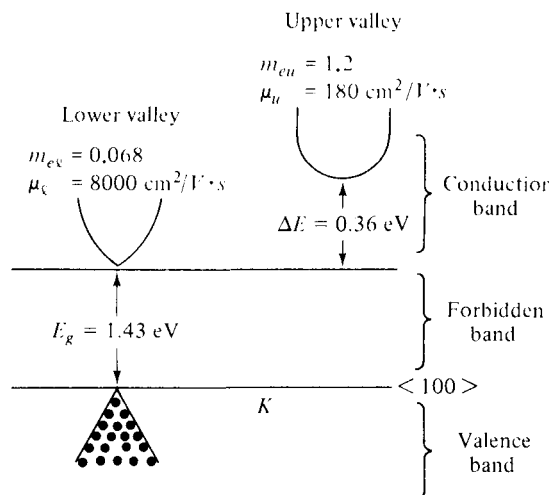


**Figure 7-2-4** Two-valley model of electron energy versus wave number for *n*-type GaAs.

**TABLE 7-2-1** DATA FOR TWO VALLEYS IN GaAs

Valley	Effective Mass $M_e$	Mobility $\mu$	Separation $\Delta E$
Lower	$M_{el} = 0.068$	$\mu_e = 8000 \text{ cm}^2/\text{V}\cdot\text{sec}$	$\Delta E = 0.36 \text{ eV}$
Upper	$M_{eu} = 1.2$	$\mu_u = 180 \text{ cm}^2/\text{V}\cdot\text{sec}$	$\Delta E = 0.36 \text{ eV}$

the data for the two valleys in the *n*-type GaAs and Table 7-2-2 shows the data for two-valley semiconductors.

Electron densities in the lower and upper valleys remain the same under an equilibrium condition. When the applied electric field is lower than the electric field of the lower valley ( $E < E_\ell$ ), no electrons will transfer to the upper valley as shown in Fig. 7-2-5(a). When the applied electric field is higher than that of the lower valley and lower than that of the upper valley ( $E_\ell < E < E_u$ ), electrons will begin to transfer to the upper valley as shown in Fig. 7-2-5(b). And when the applied electric

**TABLE 7-2-2** DATA FOR TWO-VALLEY SEMICONDUCTORS

Semiconductor	Gap energy (at 300°K) $E_g(\text{eV})$	Separation energy between two valleys $\Delta E(\text{eV})$	Threshold field $E_{th}(\text{KV/cm})$	Peak velocity $v_p(10^7 \text{ cm/s})$
Ge	0.80	0.18	2.3	1.4
GaAs	1.43	0.36	3.2	2.2
InP	1.33	0.60	10.5	2.5
		0.80		
CdTe	1.44	0.51	13.0	1.5
InAs	0.33	1.28	1.60	3.6
InSb	0.16	0.41	0.6	5.0

*Note:* InP is a three-valley semiconductor: 0.60 eV is the separation energy between the middle and lower valleys, 0.8 eV that between the upper and lower valleys.

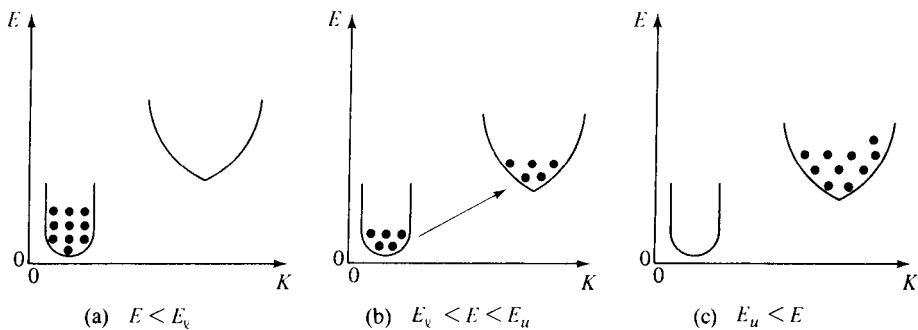


Figure 7-2-5 Transfer of electron densities.

field is higher than that of the upper valley ( $E_u < E$ ), all electrons will transfer to the upper valley as shown in Fig. 7-2-5(c).

If electron densities in the lower and upper valleys are  $n_e$  and  $n_u$ , the conductivity of the  $n$ -type GaAs is

$$\sigma = e(\mu_e n_e + \mu_u n_u) \quad (7-2-2)$$

where  $e$  = the electron charge

$\mu$  = the electron mobility

$n = n_e + n_u$  is the electron density

#### Example 7-2-1: Conductivity of an $n$ -Type GaAs Gunn Diode

Electron density:

$$n = 10^{18} \text{ cm}^{-3}$$

Electron density at lower valley:

$$n_e = 10^{10} \text{ cm}^{-3}$$

Electron density at upper valley:

$$n_u = 10^8 \text{ cm}^{-3}$$

Temperature:

$$T = 300^\circ\text{K}$$

Determine the conductivity of the diode.

**Solution** From Eq. (7-2-2) the conductivity is

$$\begin{aligned} \sigma &= e(\mu_e n_e + \mu_u n_u) \\ &= 1.6 \times 10^{-19} (8000 \times 10^{-4} \times 10^{16} + 180 \times 10^{-4} \times 10^{14}) \\ &\simeq 1.6 \times 10^{-19} \times 8000 \times 10^{-4} \times 10^{16} \quad \text{for } n_e \gg n_u \\ &= 1.28 \text{ mmhos} \end{aligned}$$

When a sufficiently high field  $E$  is applied to the specimen, electrons are accelerated and their effective temperature rises above the lattice temperature. Furthermore, the lattice temperature also increases. Thus electron density  $n$  and mobility  $\mu$  are both functions of electric field  $E$ . Differentiation of Eq. (7-2-2) with respect to  $E$  yields

$$\frac{d\sigma}{dE} = e \left( \mu_e \frac{dn_e}{dE} + \mu_u \frac{dn_u}{dE} \right) + e \left( n_e \frac{d\mu_e}{dE} + n_u \frac{d\mu_u}{dE} \right) \quad (7-2-3)$$

If the total electron density is given by  $n = n_e + n_u$  and it is assumed that  $\mu_e$  and  $\mu_u$  are proportional to  $E^p$ , where  $p$  is a constant, then

$$\frac{d}{dE} (n_e + n_u) = \frac{dn}{dE} = 0 \quad (7-2-4)$$

$$\frac{dn_e}{dE} = -\frac{dn_u}{dE} \quad (7-2-5)$$

and  $\frac{d\mu}{dE} \propto \frac{dE^p}{dE} = pE^{p-1} = p\frac{E^p}{E} \propto p\frac{\mu}{E} = \mu\frac{p}{E}$  (7-2-6)

Substitution of Eqs. (7-2-4) to (7-2-6) into Eq. (7-2-3) results in

$$\frac{d\sigma}{dE} = e(\mu_e - \mu_u) \frac{dn_e}{dE} + e(n_e \mu_e + n_u \mu_u) \frac{p}{E} \quad (7-2-7)$$

Then differentiation of Ohm's law  $J = \sigma E$  with respect to  $E$  yields

$$\frac{dJ}{dE} = \sigma + \frac{d\sigma}{dE} E \quad (7-2-8)$$

Equation (7-2-8) can be rewritten

$$\frac{1}{\sigma} \frac{dJ}{dE} = 1 + \frac{d\sigma/dE}{\sigma/E} \quad (7-2-9)$$

Clearly, for negative resistance, the current density  $J$  must decrease with increasing field  $E$  or the ratio of  $dJ/dE$  must be negative. Such would be the case only if the right-hand term of Eq. (7-2-9) is less than zero. In other words, the condition for negative resistance is

$$-\frac{d\sigma/dE}{\sigma/E} > 1 \quad (7-2-10)$$

Substitution of Eqs. (7-2-2) and (7-2-7) with  $f = n_u/n_e$  results in [2]

$$\left[ \left( \frac{\mu_e - \mu_u}{\mu_e + \mu_u f} \right) \left( -\frac{E}{n_e} \frac{dn_e}{dE} \right) - p \right] > 1 \quad (7-2-11)$$

Note that the field exponent  $p$  is a function of the scattering mechanism and should be negative and large. This factor makes impurity scattering quite undesirable because when it is dominant, the mobility rises with an increasing field and thus  $p$  is positive. When lattice scattering is dominant, however,  $p$  is negative and must depend on the lattice and carrier temperature. The first bracket in Eq. (7-2-11) must be positive in order to satisfy inequality. This means that  $\mu_e > \mu_u$ . Electrons must begin in a low-mass valley and transfer to a high-mass valley when they are heated by the electric field. The maximum value of this term is unity—that is,  $\mu_e \gg \mu_u$ . The factor  $dn_e/dE$  in the second bracket must be negative. This quantity represents the rate of the carrier density with field at which electrons transfer to the upper valley; this rate depends on differences between electron densities, electron temperature, and gap energies in the two valleys.

On the basis of the Ridley–Watkins–Hilsum theory as described earlier, the band structure of a semiconductor must satisfy three criteria in order to exhibit negative resistance [12].

1. The separation energy between the bottom of the lower valley and the bottom of the upper valley must be several times larger than the thermal energy (about 0.026 eV) at room temperature. This means that  $\Delta E > kT$  or  $\Delta E > 0.026$  eV.
2. The separation energy between the valleys must be smaller than the gap energy between the conduction and valence bands. This means that  $\Delta E < E_g$ . Otherwise the semiconductor will break down and become highly conductive before the electrons begin to transfer to the upper valleys because hole-electron pair formation is created.
3. Electrons in the lower valley must have high mobility, small effective mass, and a low density of state, whereas those in the upper valley must have low mobility, large effective mass, and a high density of state. In other words, electron velocities ( $dE/dk$ ) must be much larger in the lower valleys than in the upper valleys.

The two most useful semiconductors—silicon and germanium—do not meet all these criteria. Some compound semiconductors, such as gallium arsenide (GaAs), indium phosphide (InP), and cadmium telluride (CdTe) do satisfy these criteria. Others such as indium arsenide (InAs), gallium phosphide (GaP), and indium antimonide (InSb) do not. Figure 7-2-6 shows a possible current versus field characteristic of a two-valley semiconductor.

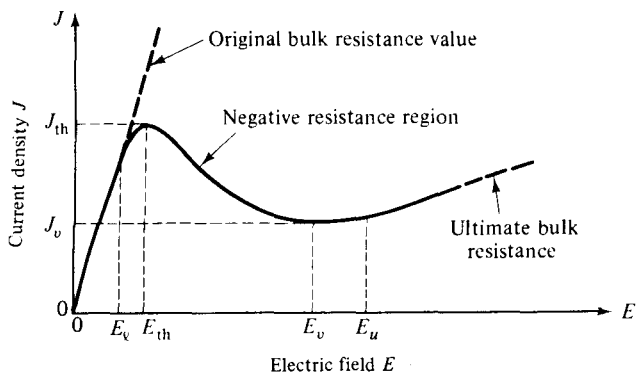


**Figure 7-2-6** Current versus field characteristic of a two-valley semiconductor.

A mathematical analysis of differential negative resistance requires a detailed analysis of high-field carrier transports [13–14]. From electric field theory the magnitude of the current density in a semiconductor is given by

$$J = qnv \quad (7-2-12)$$

where  $q$  = electric charge

$n$  = electron density, and

$v$  = average electron velocity.

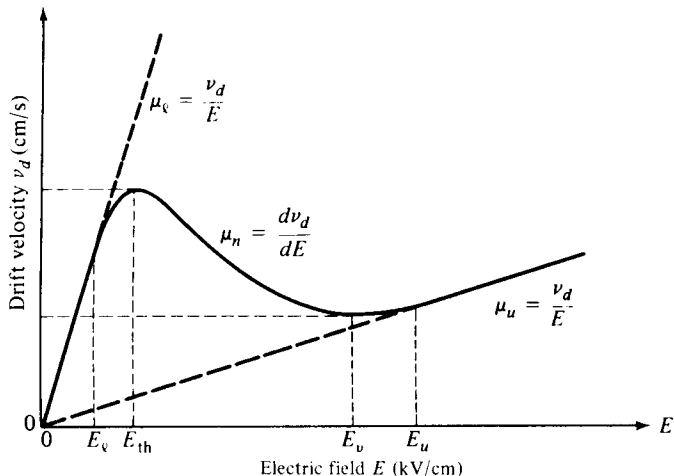


**Figure 7-2-7** Electron drift velocity versus electric field.

Differentiation of Eq. (7-2-12) with respect to electric field  $E$  yields

$$\frac{dJ}{dE} = qn \frac{dv}{dE} \quad (7-2-13)$$

The condition for negative differential conductance may then be written

$$\frac{dv_d}{dE} = \mu_n < 0 \quad (7-2-14)$$

where  $\mu_n$  denotes the negative mobility, which is shown in Fig. 7-2-7.

The direct measurement of the dependence of drift velocity on the electric field and direct evidence for the existence of the negative differential mobility were made by Ruch and Kino [15]. Experimental results, along with the theoretical results of analysis by Butcher and Fawcett [13], are shown in Fig. 7-2-8.

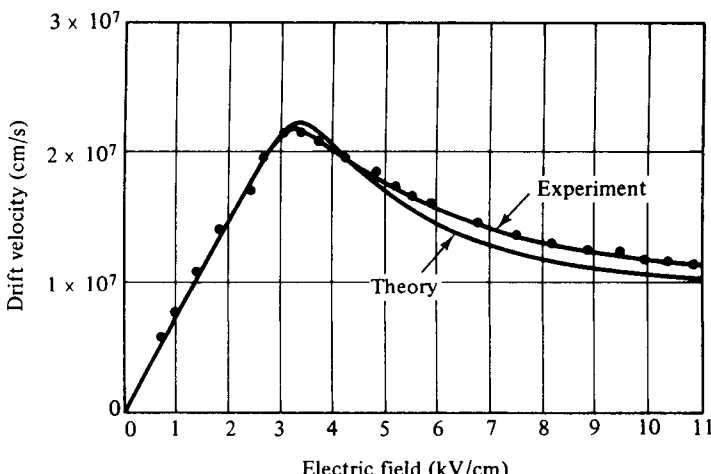


**Figure 7-2-8** Theoretical and experimental velocity-field characteristics of a GaAs diode.

**Example 7-2-2: Characteristics of a GaAs Gunn Diode**

A typical *n*-type GaAs Gunn diode has the following parameters:

Threshold field	$E_{th} = 2800 \text{ V/cm}$
Applied field	$E = 3200 \text{ V/cm}$
Device length	$L = 10 \mu\text{m}$
Doping concentration	$n_0 = 2 \times 10^{14} \text{ cm}^{-3}$
Operating frequency	$f = 10 \text{ GHz}$

- Compute the electron drift velocity.
- Calculate the current density.
- Estimate the negative electron mobility.

**Solution**

- The electron drift velocity is

$$v_d = 10 \times 10^9 \times 10 \times 10^{-6} = 10^5 \text{ m/sec} = 10^7 \text{ cm/sec}$$

- From Eq. (7-2-12) the current density is

$$\begin{aligned} J &= qnv = 1.6 \times 10^{-19} \times 2 \times 10^{20} \times 10 \times 10^9 \times 10^{-5} \\ &= 3.2 \times 10^6 \text{ A/m}^2 \\ &= 320 \text{ A/cm}^2 \end{aligned}$$

- The negative electron mobility is

$$\mu_n = -\frac{v_d}{E} = -\frac{10^7}{3200} = -3100 \text{ cm}^2/\text{V}\cdot\text{sec}$$

**7-2-3 High-Field Domain**

In the last section we described how differential resistance can occur when an electric field of a certain range is applied to a multivalley semiconductor compound, such as the *n*-type GaAs. In this section we demonstrate how a decrease in drift velocity with increasing electric field can lead to the formation of a high-field domain for microwave generation and amplification.

In the *n*-type GaAs diode the majority carriers are electrons. When a small voltage is applied to the diode, the electric field and conduction current density are uniform throughout the diode. At low voltage the GaAs is ohmic, since the drift velocity of the electrons is proportional to the electric field. This situation was shown in Fig. 7-1-2. The conduction current density in the diode is given by

$$\mathbf{J} = \sigma \mathbf{E}_x = \frac{\sigma V}{L} \mathbf{U}_x = \rho v_x \mathbf{U}_x \quad (7-2-15)$$

where  $\mathbf{J}$  = conduction current density

$\sigma$  = conductivity

$\mathbf{E}_x$  = electric field in the *x* direction

$L$  = length of the diode

$V$  = applied voltage

$\rho$  = charge density

$v$  = drift velocity

$\mathbf{U}$  = unit vector

The current is carried by free electrons that are drifting through a background of fixed positive charge. The positive charge, which is due to impurity atoms that have donated an electron (donors), is sometimes reduced by impurity atoms that have accepted an electron (acceptors). As long as the fixed charge is positive, the semiconductor is  $n$  type, since the principal carriers are the negative charges. The density of donors less the density of acceptors is termed *doping*. When the space charge is zero, the carrier density is equal to the doping.

When the applied voltage is above the threshold value, which was measured at about 3000 V/cm times the thickness of the GaAs diode, a high-field domain is formed near the cathode that reduces the electric field in the rest of the material and causes the current to drop to about two-thirds of its maximum value. This situation occurs because the applied voltage is given by

$$V = - \int_0^L E_x dx \quad (7-2-16)$$

For a constant voltage  $V$  an increase in the electric field within the specimen must be accompanied by a decrease in the electric field in the rest of the diode. The high-field domain then drifts with the carrier stream across the electrodes and disappears at the anode contact. When the electric field increases, the electron drift velocity decreases and the GaAs exhibits negative resistance.

Specifically, it is assumed that at point  $A$  on the  $J-E$  plot as shown in Fig. 7-2-9(b) there exists an excess (or accumulation) of negative charge that could be caused by a random noise fluctuation or possibly by a permanent nonuniformity in doping in the  $n$ -type GaAs diode. An electric field is then created by the accumulated charges as shown in Fig. 7-2-9(d). The field to the left of point  $A$  is lower than that to the right. If the diode is biased at point  $E_A$  on the  $J-E$  curve, this situation implies that the carriers (or current) flowing into point  $A$  are greater than those flowing out of point  $A$ , thereby increasing the excess negative space charge at  $A$ . Furthermore, when the electric field to the left of point  $A$  is lower than it was before, the field to the right is then greater than the original one, resulting in an even greater space-charge accumulation. This process continues until the low and high fields both reach values outside the differential negative-resistance region and settle at points 1 and 2 in Fig. 7-2-9(a) where the currents in the two field regions are equal. As a result of this process, a traveling space-charge accumulation is formed. This process, of course, depends on the condition that the number of electrons inside the crystal is large enough to allow the necessary amount of space charge to be built up during the transit time of the space-charge layer.

The pure accumulation layer discussed above is the simplest form of space-charge instability. When positive and negative charges are separated by a small distance, then a dipole domain is formed as shown in Fig. 7-2-10. The electric field in-

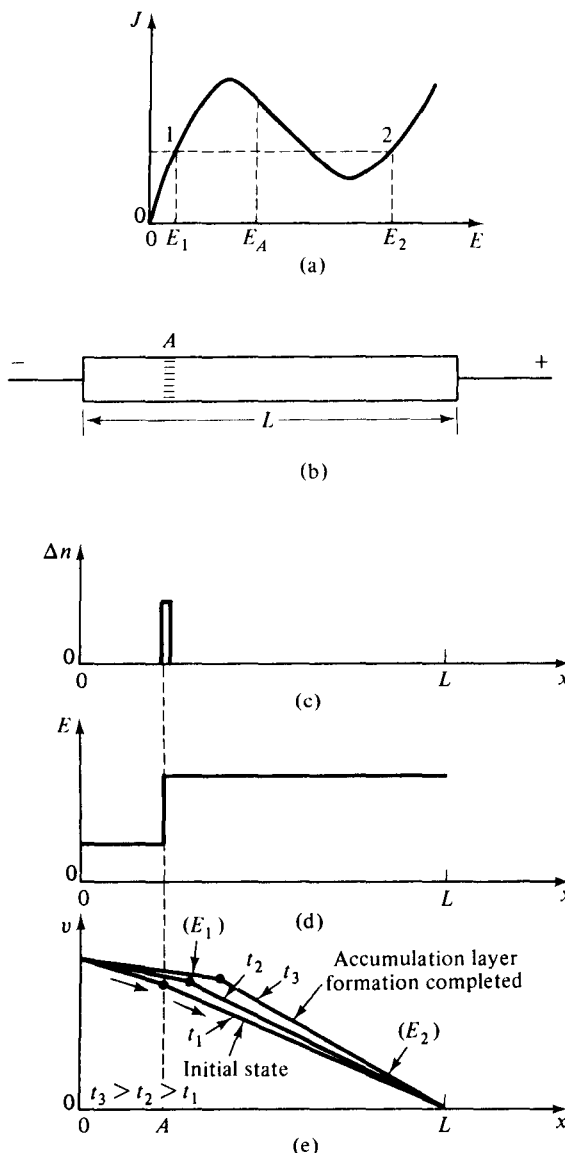


**Figure 7-2-9** Formation of an electron accumulation layer in GaAs. (After H. Kroemer [16]; reprinted by permission of IEEE, Inc.)

side the dipole domain would be greater than the fields on either side of the dipole in Fig. 7-2-10(c). Because of the negative differential resistance, the current in the low-field side would be greater than that in the high-field side. The two field values will tend toward equilibrium conditions outside the differential negative-resistance region, where the low and high currents are the same as described in the previous section. Then the dipole field reaches a stable condition and moves through the specimen toward the anode. When the high-field domain disappears at the anode, a new dipole field starts forming at the cathode and the process is repeated.

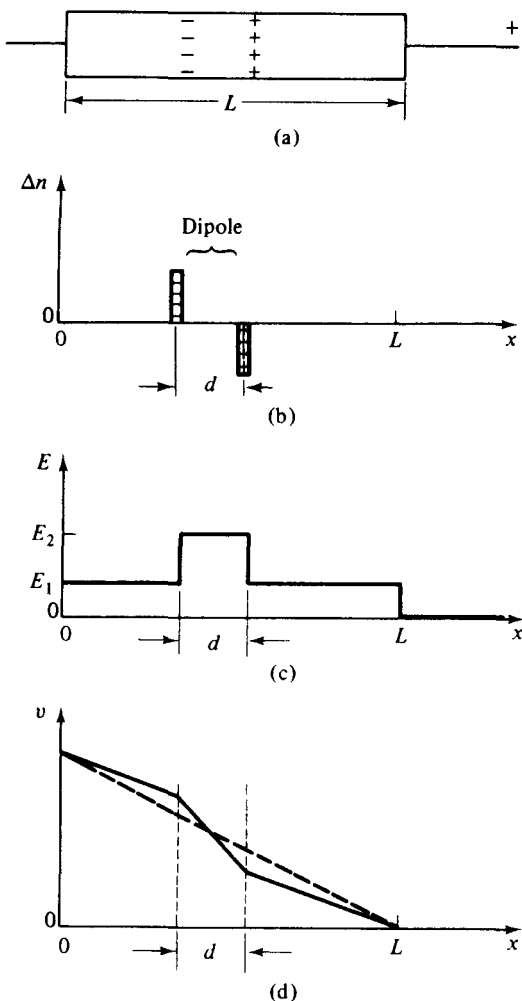


**Figure 7-2-10** Formation of an electron dipole layer in GaAs. (After H. Kroemer [16]; reprinted by permission of IEEE, Inc.)

In general, the high-field domain has the following properties [12]:

1. A domain will start to form whenever the electric field in a region of the sample increases above the threshold electric field and will drift with the carrier stream through the device. When the electric field increases, the electron drift velocity decreases and the GaAs diode exhibits negative resistance.
2. If additional voltage is applied to a device containing a domain, the domain will increase in size and absorb more voltage than was added and the current will decrease.
3. A domain will not disappear before reaching the anode unless the voltage is dropped appreciably below threshold (for a diode with uniform doping and area).

4. The formation of a new domain can be prevented by decreasing the voltage slightly below threshold (in a nonresonant circuit).
5. A domain will modulate the current through a device as the domain passes through regions of different doping and cross-sectional area, or the domain may disappear. The effective doping may be varied in regions along the drift path by additional contacts.
6. The domain's length is generally inversely proportional to the doping; thus devices with the same product of doping multiplied by length will behave similarly in terms of frequency multiplied by length, voltage/length, and efficiency.
7. As a domain passes a point in the device, the domain can be detected by a capacitive contact, since the voltage changes suddenly as the domain passes. The presence of a domain anywhere in a device can be detected by a decreased current or by a change in differential impedance.

It should be noted that properties 3 and 6 are valid only when the length of the domain is much longer than the thermal diffusion length for carriers, which for GaAs is about  $1 \mu\text{m}$  for a doping of  $10^{16}$  per cubic centimeter and about  $10 \mu\text{m}$  for a doping of  $10^{14}$  per cubic centimeter.

### 7-3 MODES OF OPERATION

Since Gunn first announced his observation of microwave oscillation in the *n*-type GaAs and *n*-type InP diodes in 1963, various modes of operation have been developed, depending on the material parameters and operating conditions. As noted, the formation of a strong space-charge instability depends on the conditions that enough charge is available in the crystal and that the specimen is long enough so that the necessary amount of space charge can be built up within the transit time of the electrons. This requirement sets up a criterion for the various modes of operation of bulk negative-differential-resistance devices. Copeland proposed four basic modes of operation of uniformly doped bulk diodes with low-resistance contacts [17] as shown in Fig. 7-3-1.

1. Gunn oscillation mode: This mode is defined in the region where the product of frequency multiplied by length is about  $10^7 \text{ cm/s}$  and the product of doping multiplied by length is greater than  $10^{12}/\text{cm}^2$ . In this region the device is unstable because of the cyclic formation of either the accumulation layer or the high-field domain. In a circuit with relatively low impedance the device operates in the high-field domain mode and the frequency of oscillation is near the intrinsic frequency. When the device is operated in a relatively high-*Q* cavity and coupled properly to the load, the domain is quenched or delayed (or both) before nucleating. In this case, the oscillation frequency is almost entirely determined by the resonant frequency of the cavity and has a value of several times the intrinsic frequency.

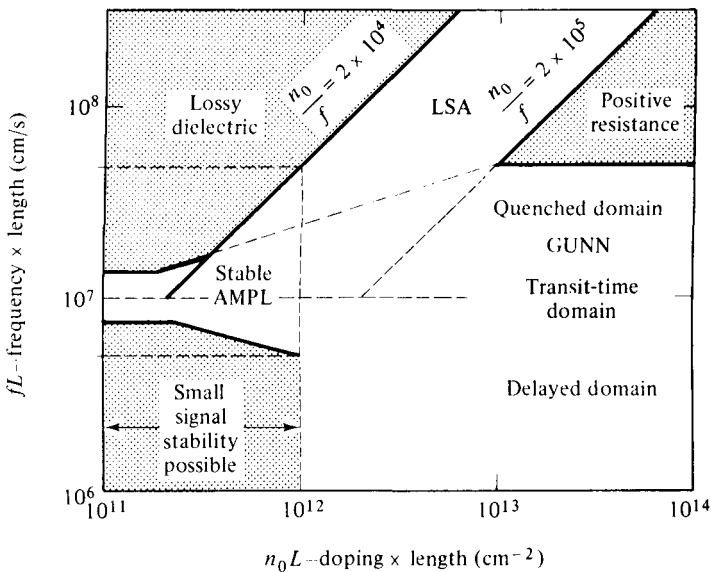


**Figure 7-3-1** Modes of operation for Gunn diodes. (After J. A. Copeland [17]; reprinted by permission of IEEE, Inc.)

2. Stable amplification mode: This mode is defined in the region where the product of frequency times length is about  $10^7$  cm/s and the product of doping times length is between  $10^{11}$  and  $10^{12}/\text{cm}^2$ .
3. LSA oscillation mode: This mode is defined in the region where the product of frequency times length is above  $10^7$  cm/s and the quotient of doping divided by frequency is between  $2 \times 10^4$  and  $2 \times 10^5$ .
4. Bias-circuit oscillation mode: This mode occurs only when there is either Gunn or LSA oscillation, and it is usually at the region where the product of frequency times length is too small to appear in the figure. When a bulk diode is biased to threshold, the average current suddenly drops as Gunn oscillation begins. The drop in current at the threshold can lead to oscillations in the bias circuit that are typically 1 kHz to 100 MHz [18].

The first three modes are discussed in detail in this section. Before doing so, however, let us consider the criterion for classifying the modes of operation.

### 7-3-1 Criterion for Classifying the Modes of Operation

The Gunn-effect diodes are basically made from an  $n$ -type GaAs, with the concentrations of free electrons ranging from  $10^{14}$  to  $10^{17}$  per cubic centimeter at room temperature. Its typical dimensions are  $150 \times 150 \mu\text{m}$  in cross section and  $30 \mu\text{m}$  long. During the early stages of space-charge accumulation, the time rate of growth

of the space-charge layers is given by

$$Q(X, t) = Q(X - vt, 0) \exp\left(\frac{t}{\tau_d}\right) \quad (7-3-1)$$

where  $\tau_d = \frac{\epsilon}{\sigma} = \frac{\epsilon}{en_0|\mu_n|}$  is the magnitude of the negative dielectric relaxation time

$\epsilon$  = semiconductor dielectric permittivity

$n_0$  = doping concentration

$\mu_n$  = negative mobility

$e$  = electron charge

$\sigma$  = conductivity

Figure 7-3-2 clarifies Eq. (7-3-1).

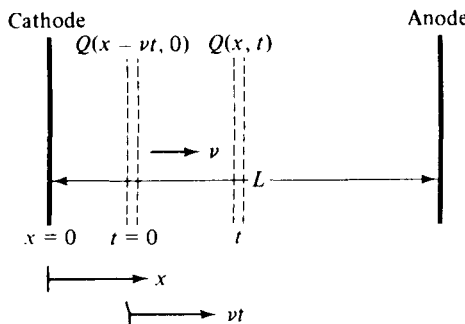


Figure 7-3-2 Space-charge accumulation with a velocity of  $v$ .

If Eq. (7-3-1) remains valid throughout the entire transit time of the space-charge layer, the factor of maximum growth is given by

$$\text{Growth factor} = \frac{Q(L, L/v)}{Q(0, 0)} = \exp\left(\frac{L}{v\tau_d}\right) = \exp\left(\frac{Ln_0e|\mu_n|}{\epsilon v}\right) \quad (7-3-2)$$

In Eq. (7-3-2) the layer is assumed to start at the cathode at  $t = 0$ ,  $X = 0$ , and arrive at the anode at  $t = L/v$  and  $X = L$ . For a large space-charge growth, this factor must be larger than unity. This means that

$$n_0 L > \frac{\epsilon v}{e|\mu_n|} \quad (7-3-3)$$

This is the criterion for classifying the modes of operation for the Gunn-effect diodes. For  $n$ -type GaAs, the value of  $\epsilon v/(e|\mu_n|)$  is about  $10^{12}/\text{cm}^2$ , where  $|\mu_n|$  is assumed to be  $150 \text{ cm}^2/\text{V} \cdot \text{s}$ .

### Example 7-3-1: Criterion of Mode Operation

An  $n$ -type GaAs Gunn diode has the following parameters:

Electron drift velocity:  $v_d = 2.5 \times 10^5 \text{ m/s}$

Negative electron mobility:  $|\mu_n| = 0.015 \text{ m}^2/\text{V} \cdot \text{s}$

Relative dielectric constant:  $\epsilon_r = 13.1$

Determine the criterion for classifying the modes of operation.

**Solution** From Eq. (7-3-3) the criterion is

$$\begin{aligned}\frac{\epsilon v_d}{e|\mu_n|} &= \frac{8.854 \times 10^{-12} \times 13.1 \times 2.5 \times 10^5}{1.6 \times 10^{-19} \times 0.015} \\ &= 1.19 \times 10^{16}/\text{m}^2 \\ &= 1.19 \times 10^{12}/\text{cm}^2\end{aligned}$$

This means that the product of the doping concentration and the device length must be

$$n_0 L > 1.19 \times 10^{12}/\text{cm}^2$$


---

### 7-3-2 Gunn Oscillation Modes ( $10^{12}/\text{cm}^2 \leq (n_0 L) < 10^{14}/\text{cm}^2$ )

Most Gunn-effect diodes have the product of doping and length ( $n_0 L$ ) greater than  $10^{12}/\text{cm}^2$ . However, the mode that Gunn himself observed had a product  $n_0 L$  that is much less. When the product of  $n_0 L$  is greater than  $10^{12}/\text{cm}^2$  in GaAs, the space-charge perturbations in the specimen increase exponentially in space and time in accordance with Eq. (7-3-1). Thus a high-field domain is formed and moves from the cathode to the anode as described earlier. The frequency of oscillation is given by the relation [19]

$$f = \frac{v_{\text{dom}}}{L_{\text{eff}}} \quad (7-3-4)$$

where  $v_{\text{dom}}$  is the domain velocity and  $L_{\text{eff}}$  is the effective length that the domain travels from the time it is formed until the time that a new domain begins to form.

Gunn described the behavior of Gunn oscillators under several circuit configurations [20]. When the circuit is mainly resistive or the voltage across the diode is constant, the period of oscillation is the time required for the domain to drift from the cathode to the anode. This mode is not actually typical of microwave applications. Negative conductivity devices are usually operated in resonant circuits, such as high- $Q$  resonant microwave cavities. When the diode is in a resonant circuit, the frequency can be tuned to a range of about an octave without loss of efficiency [21].

As described previously, the normal Gunn domain mode (or Gunn oscillation mode) is operated with the electric field greater than the threshold field ( $E > E_{\text{th}}$ ). The high-field domain drifts along the specimen until it reaches the anode or until the low-field value drops below the sustaining field  $E_s$  required to maintain  $v_s$  as shown in Fig. 7-3-3. The sustaining drift velocity for GaAs is  $v_s = 10^7 \text{ cm/s}$ . Since the electron drift velocity  $v$  varies with the electric field, there are three possible domain modes for the Gunn oscillation mode.

*Transit-time domain mode* ( $fL \approx 10^7 \text{ cm/s}$ ). When the electron drift velocity  $v_d$  is equal to the sustaining velocity  $v_s$ , the high-field domain is stable. In other words, the electron drift velocity is given by

$$v_d = v_s = fL \approx 10^7 \text{ cm/s} \quad (7-3-5)$$

Then the oscillation period is equal to the transit time—that is,  $\tau_0 = \tau_t$ . This situation is shown in Fig. 7-3-4(a). The efficiency is below 10% because the current is collected only when the domain arrives at the anode.

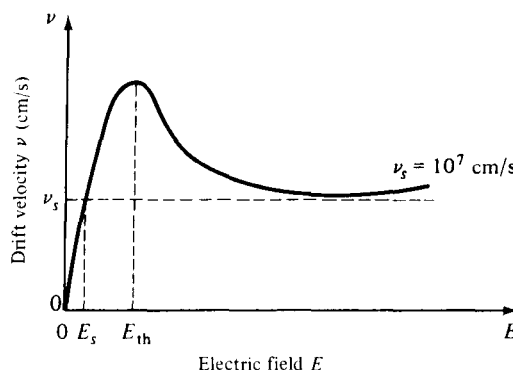


**Figure 7-3-3** Electron drift velocity versus electric field.

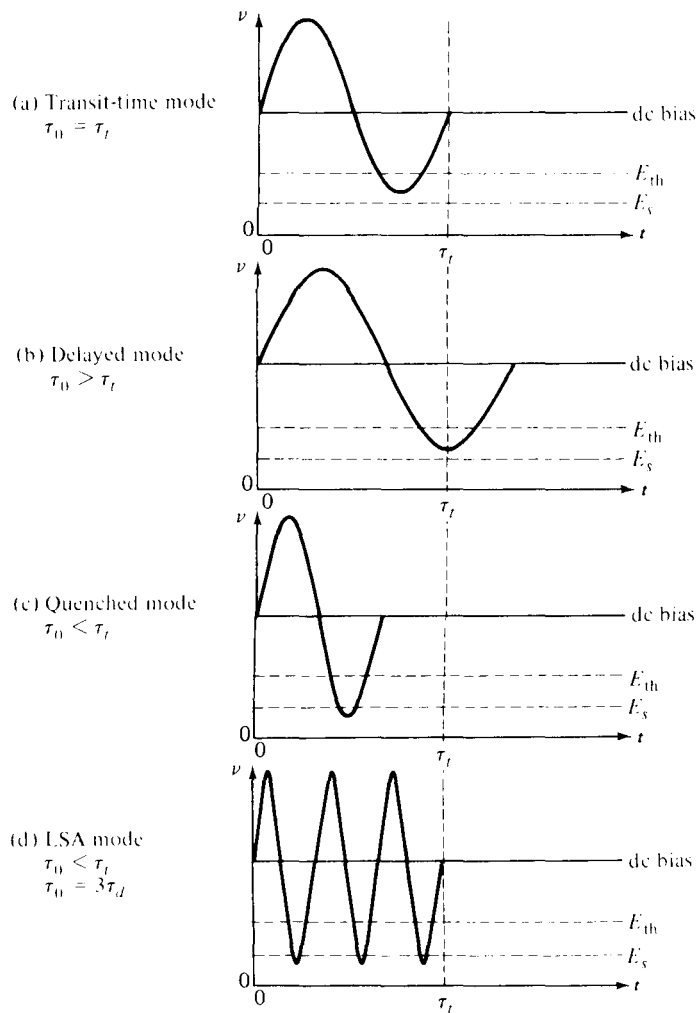


**Figure 7-3-4** Gunn domain modes.

*Delayed domain mode* ( $10^6 \text{ cm/s} < fL < 10^7 \text{ cm/s}$ ). When the transit time is chosen so that the domain is collected while  $E < E_{\text{th}}$  as shown in Fig. 7-3-4(b), a new domain cannot form until the field rises above threshold again. In this case, the oscillation period is greater than the transit time—that is,  $\tau_0 > \tau$ . This delayed mode is also called *inhibited mode*. The efficiency of this mode is about 20%.

*Quenched domain mode* ( $fL > 2 \times 10^7 \text{ cm/s}$ ). If the bias field drops below the sustaining field  $E_s$  during the negative half-cycle as shown in Fig. 7-3-4(c), the domain collapses before it reaches the anode. When the bias field swings back above threshold, a new domain is nucleated and the process repeats. Therefore the oscillations occur at the frequency of the resonant circuit rather than at the transit-time frequency. It has been found that the resonant frequency of the circuit is several times the transit-time frequency, since one dipole does not have enough time to readjust and absorb the voltage of the other dipoles [22, 23]. Theoretically, the efficiency of quenched domain oscillators can reach 13% [22].

### 7-3-3 Limited-Space-Charge Accumulation (LSA) Mode ( $fL > 2 \times 10^7 \text{ cm/s}$ )

When the frequency is very high, the domains do not have sufficient time to form while the field is above threshold. As a result, most of the domains are maintained in the negative conductance state during a large fraction of the voltage cycle. Any accumulation of electrons near the cathode has time to collapse while the signal is below threshold. Thus the LSA mode is the simplest mode of operation, and it consists of a uniformly doped semiconductor without any internal space charges. In this instance, the internal electric field would be uniform and proportional to the applied voltage. The current in the device is then proportional to the drift velocity at this field level. The efficiency of the LSA mode can reach 20%.

The oscillation period  $\tau_0$  should be no more than several times larger than the magnitude of the dielectric relaxation time in the negative conductance region  $\tau_d$ . The oscillation indicated in Fig. 7-3-4(d) is  $\tau_0 = 3\tau_d$ . It is appropriate here to define the LSA boundaries. As described earlier, the sustaining drift velocity is  $10^7 \text{ cm/s}$  as shown in Eq. (7-3-5) and Fig. 7-3-3. For the  $n$ -type GaAs, the product of doping and length ( $n_0 L$ ) is about  $10^{12}/\text{cm}^2$ . At the low-frequency limit, the drift velocity is taken to be

$$v_\ell = fL = 5 \times 10^6 \text{ cm/s} \quad (7-3-6)$$

The ratio of  $n_0 L$  to  $fL$  yields

$$\frac{n_0}{f} = 2 \times 10^5 \quad (7-3-7)$$

At the upper-frequency limit it is assumed that the drift velocity is

$$v_u = fL = 5 \times 10^7 \text{ cm/s} \quad (7-3-8)$$

and the ratio of  $n_0 L$  to  $fL$  is

$$\frac{n_0}{f} = 2 \times 10^4 \quad (7-3-9)$$

Both the upper and lower boundaries of the LSA mode are indicated in Fig. 7-3-1. The LSA mode is discussed further in Section 7-4.

### 7-3-4 Stable Amplification Mode ( $n_0 L < 10^{12}/\text{cm}^2$ )

When the  $n_0 L$  product of the device is less than about  $10^{12}/\text{cm}^2$ , the device exhibits amplification at the transit-time frequency rather than spontaneous oscillation. This situation occurs because the negative conductance is utilized without domain formation. There are too few carriers for domain formation within the transit time. Therefore amplification of signals near the transit-time frequency can be accomplished. This mode was first observed by Thim and Barber [23]. Furthermore, Uenohara showed that there are types of amplification depending on the  $fL$  product of the device [24] as shown in Fig. 7-3-5.

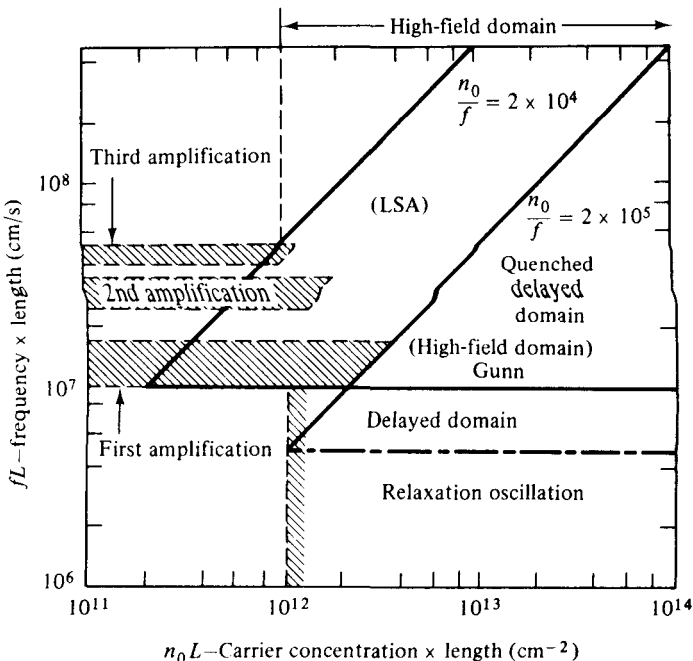


**Figure 7-3-5** Mode chart. (After M. Uenohara [24]; reprinted by permission of McGraw-Hill Book Company.)

The various modes of operation of Gunn diodes can be classified on the basis of the times in which various processes occur. These times are defined as follows:

$\tau_t$  = domain transit time

$\tau_d$  = dielectric relaxation time at low field

$\tau_g$  = domain growth time

$\tau_0$  = natural period of oscillation of a high- $Q$  external electric circuit

The modes described previously are summarized in Table 7-3-1.

**TABLE 7-3-1** MODES OF OPERATION OF GUNN OSCILLATORS

Mode	Time relationship	Doping level	Nature of circuit
Stable amplifier	$\tau_0 \geq \tau_t$	$n_0 L < 10^{12}$	Nonresonant
Gun domain	$\tau_g \leq \tau_t$	$n_0 L > 10^{12}$	Nonresonant; constant voltage
Quenched domain	$\tau_0 = \tau_t$		Resonant; finite impedance
Delayed domain	$\tau_g \leq \tau_t$ $\tau_0 > \tau_t$	$n_0 L > 10^{12}$	Resonant; finite impedance
LSA	$\tau_0 < \tau_g$ $\tau_0 > \tau_d$	$2 \times 10^4 < \left(\frac{n_0}{f}\right) < 2 \times 10^5$	Multiple resonances; high impedance; high dc bias

## 7-4 LSA DIODES

The abbreviation LSA stands for the limited space-charge accumulation mode of the Gunn diode. As described previously, if the product  $n_0 L$  is larger than  $10^{12}/\text{cm}^2$  and if the ratio of doping  $n_0$  to frequency  $f$  is within  $2 \times 10^5$  to  $2 \times 10^4 \text{ s/cm}^3$ , the high-field domains and the space-charge layers do not have sufficient time to build up. The magnitude of the RF voltage must be large enough to drive the diode below threshold during each cycle in order to dissipate space charge. Also, the portion of each cycle during which the RF voltage is above threshold must be short enough to prevent the domain formation and the space-charge accumulation. Only the primary accumulation layer forms near the cathode; the rest of the sample remains fairly homogeneous. Thus with limited space-charge formation the remainder of the sample appears as a series negative resistance that increases the frequency of the oscillations in the resonant circuit. Copeland discovered the LSA mode of the Gunn diode in 1966 [25]. In the LSA mode the diode is placed in a resonator tuned to an oscillation frequency of

$$f_0 = \frac{1}{\tau_0} \quad (7-4-1)$$

The device is biased to several times the threshold voltage (see Fig. 7-4-1).

As the RF voltage swings beyond the threshold, the space charge starts building up at the cathode. Since the oscillation period  $\tau_0$  of the RF signal is less than the domain-growth time constant  $\tau_g$ , the total voltage swings below the threshold before the domain can form. Furthermore, since  $\tau_0$  is much greater than the dielectric relaxation time  $\tau_d$ , the accumulated space charge is drained in a very small fraction of the RF cycle. Therefore the device spends most of the RF cycle in the negative-resistance region, and the space charge is not allowed to build up. The frequency of oscillation in the LSA mode is independent of the transit time of the carriers and is determined solely by the circuit external to the device. Also, the power-impedance product does not fall off as  $1/f_0^2$ ; thus the output power in the LSA mode can be greater than that in the other modes.

The LSA mode does have limitations. It is very sensitive to load conditions, temperatures, and doping fluctuations [26]. In addition, the RF circuit must allow the field to build up quickly in order to prevent domain formation. The power output

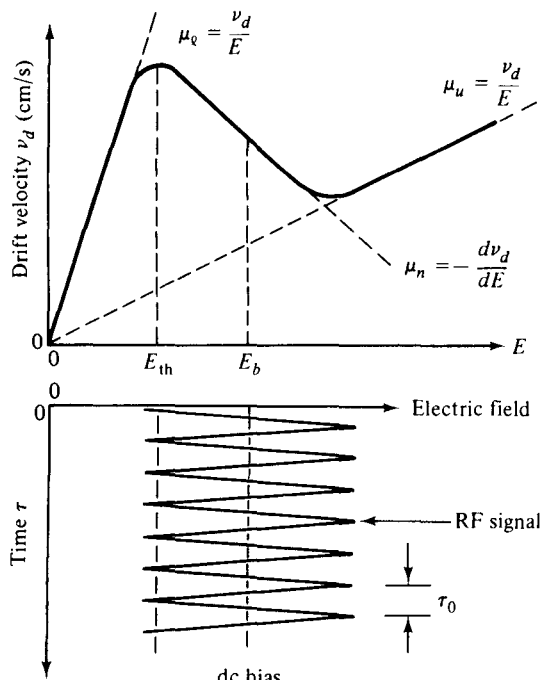


Figure 7-4-1 LSA mode operation.

of an LSA oscillator can be simply written

$$P = \eta V_0 I_0 = \eta (M E_{th} L) (n_0 e v_0 A) \quad (7-4-2)$$

where  $\eta$  = dc-to-RF conversion efficiency (primarily a function of material and circuit considerations)

$V_0$  = operating voltage

$I_0$  = operating current

$M$  = multiple of the operating voltage above negative-resistance threshold voltage

$E_{th}$  = threshold field (about 3400 V/cm)

$L$  = device length (about 10 to 200  $\mu\text{m}$ )

$n_0$  = donor concentration (about  $10^{15} \text{ e/cm}^3$ )

$e$  = electron charge ( $1.6 \times 10^{-19} \text{ C}$ )

$v_0$  = average carrier drift velocity (about  $10^7 \text{ cm/s}$ )

$A$  = device area (about  $3 \times 10^{-4}$  to  $20 \times 10^{-4} \text{ cm}^2$ )

For an LSA oscillator,  $n_0$  is primarily determined by the desired operating frequency  $f_0$  so that, for a properly designed circuit, peak power output is directly proportional to the volume ( $LA$ ) of the device length  $L$  multiplied by the area  $A$  of the active layer. Active volume cannot be increased indefinitely. In the theoretical limit, this is due to electrical wavelength and skin-depth considerations. In the practical limit, however, available bias, thermal dissipation capability, or technological problems associated with material uniformity limit device length. The power capabilities of LSA oscillators vary from 6 kW (pulse) at 1.75 GHz to 400 W (pulse) at 51 GHz.

**Example 7-4-1: Output Power of an LSA Oscillator**

An LSA oscillator has the following parameters:

Conversion efficiency:	$\eta = 0.06$
Multiplication factor:	$M = 3.5$
Threshold field:	$E_{th} = 320 \text{ kV/m}$
Device length:	$L = 12\mu\text{m}$
Donor concentration:	$n_0 = 10^{21} \text{ m}^3$
Average carrier velocity:	$v_0 = 1.5 \times 10^5 \text{ m/s}$
Area:	$A = 3 \times 10^{-8} \text{ m}^2$

Determine the output power in milliwatts.

**Solution** From Eq. (7-4-2) the output power is

$$\begin{aligned} P &= \eta(ME_{th}L)(n_0ev_0A) = 0.06 \times (3.5 \times 320 \times 10^3 \times 12 \times 10^{-6}) \\ &\quad \times (10^{21} \times 1.6 \times 10^{-19} \times 1.5 \times 10^5 \times 3 \times 10^{-8}) \\ &= 0.06 \times 13.44 \times 7.2 \times 10^{-1} = 581 \text{ mW} \end{aligned}$$

**7-5 InP DIODES**

When Gunn first announced his Gunn effect in 1963, the diodes he investigated were of gallium arsenide (GaAs) and indium phosphide (InP). The GaAs diode was described earlier in the chapter. In this section the *n*-type InP diode is discussed. Both the GaAs diode and the InP diode operate basically the same way in a circuit with dc voltage applied at the electrodes. In the ordinary Gunn effect in the *n*-type GaAs, the two-valley model theory is the foundation for explaining the electrical behavior of the Gunn effect. However, Hilsum proposed that indium phosphide and some alloys of indium gallium antimonide should work as three-level devices [27]. Figure 7-5-1 shows the three-valley model for indium phosphide.

It can be seen that InP, besides having an upper-valley energy level and a lower-valley energy level similar to the model shown in Fig. 7-2-4 for *n*-type GaAs, also has a third middle-valley energy level. In GaAs the electron transfer process from the lower valley to the upper valley is comparatively slow. At a particular voltage above threshold current flow consists of a larger contribution of electrons from the lower valley rather than from the upper valley. Because of this larger contribution from the lower-energy level, a relatively low peak-to-valley current ratio results, which is shown in Fig. 7-5-2.

As shown in Fig. 7-5-3, the InP diode has a larger peak-to-valley current ratio because an electron transfer proceeds rapidly as the field increases. This situation occurs because the coupling between the lower valley and upper valley in InP is weaker than in GaAs. The middle-valley energy level provides the additional energy loss mechanism required to avoid breakdown caused by the high energies acquired by the lower-valley electrons from the weak coupling. It can be seen from Fig. 7-5-1

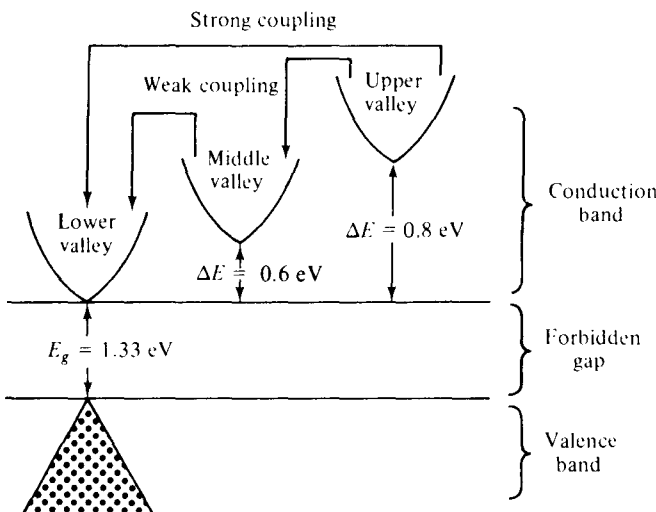


**Figure 7-5-1** Three-valley-model energy level for InP diode.

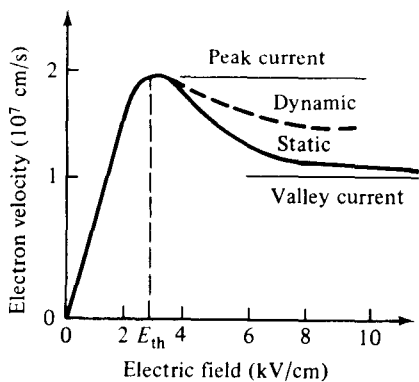


**Figure 7-5-2** Peak-to-valley current ratio for *n*-type GaAs.

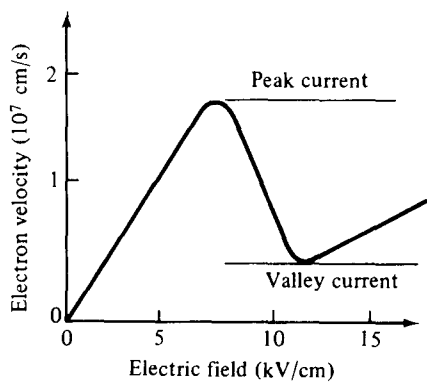


**Figure 7-5-3** Peak-to-valley current ratio for InP.

that the lower valley is weakly coupled to the middle valley but strongly coupled to the upper valley to prevent breakdown. This situation ensures that under normal operating conditions electrons concentrate in the middle valley. Because InP has a greater energy separation between the lower valley and the nearest energy levels, the thermal excitation of electrons has less effect, and the degradation of its peak-to-valley current ratio is about four times less than in GaAs [28].

The mode of operation of InP is unlike the domain oscillating mode in which a high-field domain is formed that propagates with a velocity of about  $10^7 \text{ cm/s}$ . As a result, the output current waveform of an InP diode is transit-time dependent. This mode reduces the peak-to-valley current ratio so that efficiency is reduced. For this

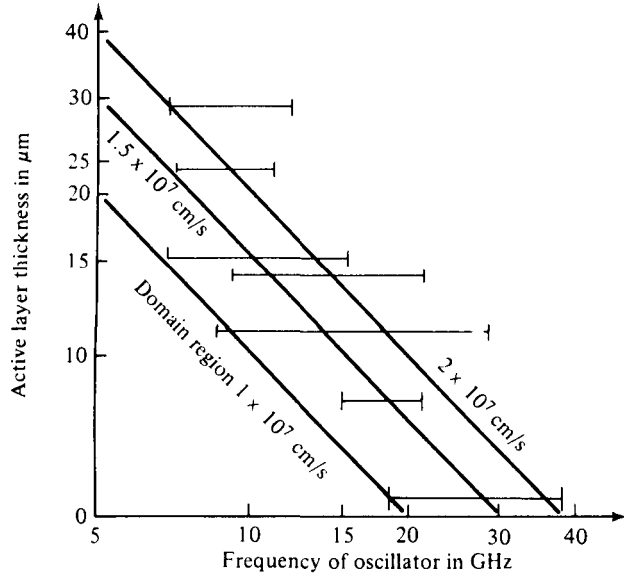


**Figure 7-5-4** Active-layer thickness versus frequency for InP diode. (From B. C. Taylor and D. J. Colliver [29]; reprinted by permission of IEEE, Inc.)

reason, an operating mode is usually sought where charge domains are not formed. The three-valley model of InP inhibits the formation of domains because the electron diffusion coefficient is increased by the stronger coupling [28]. From experiments performed by Taylor and Colliver [29] it was determined that epitaxial InP oscillators operate through a transit-time phenomenon and do not oscillate in a bulk mode of the LSA type. From their findings it was determined that it is not appropriate to attempt to describe the space-charge oscillations in InP in terms of modes known to exist in GaAs devices. Taylor and Colliver also determined that the frequencies obtained from a device were dependent on the active-layer thickness. The InP oscillator could be tuned over a large frequency range, bounded only by the thickness, by adjusting the cavity size. Figure 7-5-4 shows the frequency ranges for the different active-layer thicknesses and lines of constant electron velocity [28, 29]. It can be seen from the figure that only a few InP devices operate in the domain formation area. In each case on the graph, the maximum efficiency occurs at about midband [29]. Table 7-5-1 summarizes the highest power and efficiencies for InP diodes.

**TABLE 7-5-1** BEST PERFORMANCE OF InP DIODE

Frequency (GHz)	Thickness (μm)	Power (W)	Operation	Efficiency (%)	Reference
5.5	—	3.05	pulsed	14.7	[28]
8.5	28	0.95	pulsed	7.0	[29]
10.75	—	1.33	pulsed	12.0	[28]
13.8	11	0.50	pulsed	6.3	[29]
15	—	1.13	pulsed	15	[28]
18	11	1.05	pulsed	4.2	[29]
18	—	0.20	CW	10.2	[28]
25	5.4	0.65	pulsed	2.6	[29]
26	—	0.15	CW	6	[28]
29.4	5.4	0.23	pulsed	2	[29]
33	5.4	0.10	pulsed	0.4	[29]
37	—	0.01	CW	1	[28]

## 7-6 CdTe DIODES

The Gunn effect, first observed by Gunn as a time variation in the current through samples of *n*-type GaAs when the voltage across the sample exceeded a critical value, has since been observed in *n*-type InP, *n*-type CdTe, alloys of *n*-GaAs and *n*-GaP, and in InAs. In *n*-type cadmium telluride (CdTe), the Gunn effect was first seen by Foyt and McWhorter [30], who observed a time variation of the current through samples 250 to 300  $\mu\text{m}$  long with a carrier concentration of  $5 \times 10^{14}/\text{cm}^3$  and a room temperature mobility of  $1000 \text{ cm}^2/\text{V} \cdot \text{s}$ . Ludwig, Halsted, and Aven [31] confirmed the existence of current oscillations in *n*-CdTe, and Ludwig has further reported studies of the Gunn effect in CdTe over a wider range of sample doping levels and lengths [32]. It has been confirmed that the same mechanism—the field-induced transfer of electrons to a higher conduction band minimum (Gunn effect)—applies in CdTe just as it does in GaAs. From the two-valley model theory in CdTe, as in GaAs, the  $\langle 000 \rangle$  minimum is the lowest in energy. The effective mass  $m_{\text{eff}} = 0.11 m$  (electron mass) and the intrinsic mobility  $\mu \approx 1100 \text{ cm}^2/\text{V} \cdot \text{s}$  at room temperature. Hilsum has estimated that  $\langle 111 \rangle$  minima are the next lowest in energy, being 0.51 eV higher than  $\langle 000 \rangle$  minimum [33]. In comparing the Gunn effect in CdTe to that in GaAs, a major difference is the substantially higher threshold field, about 13 kV/cm for CdTe compared with about 3 kV/cm for GaAs [34]. Qualitatively, the higher threshold can be thought of as associated with the relatively strong coupling of the electrons to longitudinal optical phonons, which limits the mobility—and hence the rate of energy acquisition from the applied field—and also provides an efficient mechanism for transferring energy to the lattice, thereby minimizing the kinetic energy in the electron distribution.

The ratio of peak-to-valley current is another parameter of interest. In CdTe, as in GaAs, the spike amplitude can be as large as 50% of the maximum total current. A similar maximum efficiency for CdTe and GaAs can be expected. Since the domain velocities in CdTe and GaAs are approximately equal, samples of the same length will operate at about the same frequency in the transit-time mode. The high threshold field of CdTe combined with its poor thermal conductivity creates a heating problem. If sufficiently short pulses are used so that the heat can be dissipated, however, the high operating field of the sample can be an advantage.

## 7-7 MICROWAVE GENERATION AND AMPLIFICATION

### 7-7-1 Microwave Generation

As described earlier in this section, if the applied field is less than threshold the specimen is stable. If, however, the field is greater than threshold, the sample is unstable and divides up into two domains of different conductivity and different electric field but the same drift velocity. Figure 7-7-1 shows the stable and unstable regions.

At the initial formation of the accumulation layer, the field behind the layer decreases and the field in front of it increases. This process continues as the layer travels from the cathode toward the anode. As the layer approaches the anode, the field

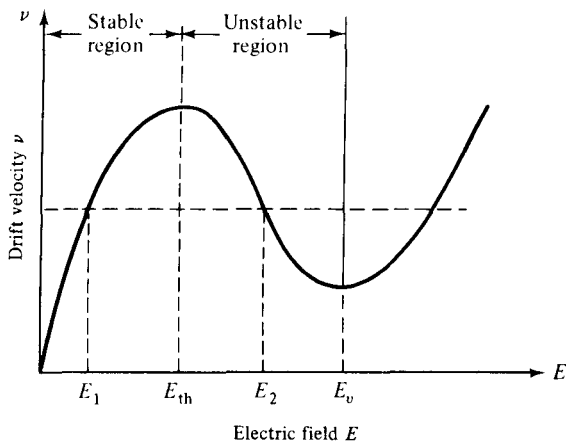


**Figure 7-7-1** Electric field versus drift velocity.

behind it begins to increase again; and after the layer is collected by the anode, the field in the whole sample is higher than threshold. When the high-field domain disappears at the anode, a new dipole field starts forming again at the cathode and the process repeats itself. Since current density is proportional to the drift velocity of the electrons, a pulsed current output is obtained. The oscillation frequency of the pulsed current is given by

$$f = \frac{v_d}{L_{\text{eff}}} \quad (7-7-1)$$

where  $v_d$  is the velocity of the domain or approximately the drift velocity of the electrons and  $L_{\text{eff}}$  is the effective length that the domain travels. Experiments have shown that the  $n$ -type GaAs diodes have yielded 200-W pulses at 3.05 GHz and 780-mW CW power at 8.7 GHz. Efficiencies of 29% have been obtained in pulsed operation at 3.05 GHz and 5.2% in CW operation at 24.8 GHz. Predictions have been made that 250-kW pulses from a single block of  $n$ -type GaAs are theoretically possible up to 100 GHz.

The source generation of solid-state microwave devices has many advantages over the vacuum tube devices they are beginning to replace. However, at present they also have serious drawbacks that could prevent more widespread application. The most important disadvantages are:

1. Low efficiency at frequencies above 10 GHz
2. Small tuning range
3. Large dependence of frequency on temperature
4. High noise

These problems are common to both avalanche diodes and transferred electron devices [35].

Figure 7-7-2 shows the latest state-of-the-art performance for GaAs and InP Gunn diodes [36]. The numbers adjacent to the data points indicate efficiency in percent. Gunn diode oscillators have better noise performance than IMPATTs. They are

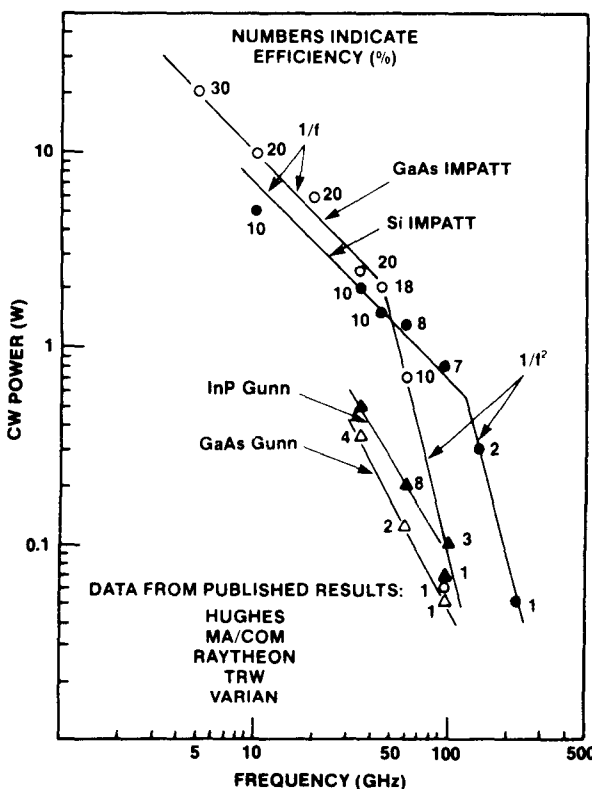


**Figure 7-7-2** State-of-the-art performance for GaAs and InP Gunn diodes. (From H. Hieslmair et al. [36]; reprinted by permission of Microwave Journal, Inc.)

used as local oscillators for receivers and as primary sources where CW powers of up to 100 mW are required. InP Gunn diodes have higher power and efficiency than GaAs Gunn diodes.

### 7-7-2 Microwave Amplification

When an RF signal is applied to a Gunn oscillator, amplification of the signal occurs, provided that the signal frequency is low enough to allow the space charge in the domain to readjust itself. There is a critical value of  $fL$  above which the device will not amplify. Below this frequency limit the sample presents an impedance with a negative real part that can be utilized for amplification. If  $n_0 L$  becomes less than  $10^{12}/\text{cm}^2$ , domain formation is inhibited and the device exhibits a nonuniform field distribution that is stable with respect to time and space. Such a diode can amplify signals in the vicinity of the transit-time frequency and its harmonics without oscillation. If this device is used in a circuit with enough positive feedback, it will oscillate. Hakki has shown that the oscillation diode can amplify at nearby frequencies or can be used simultaneously as an amplifier and local oscillator [37]. However, the output power of a stable amplifier is quite low because of the limitation imposed by the value of  $n_0 L$ .

In contrast to the stable amplifier, the Gunn-effect diode must oscillate at the transit-time frequency while it is amplifying at some other frequency. The value of  $n_0 L$  must be larger than  $10^{12}/\text{cm}^2$  in order to establish traveling domain oscillations; hence substantially larger output power can be obtained. Because of the presence of high-field domains, this amplifier is called a *traveling domain amplifier* (TDA).

Although a large number of possible amplifier circuits exist, the essential feature of each is to provide both a broadband circuit at the signal frequency and a short circuit at the Gunn oscillation frequency. In order to maintain stability with respect to the signal frequency, the Gunn diode must see a source admittance whose real part is larger than the negative conductance of the diode. The simplest circuit satisfying this condition is shown in Fig. 7-7-3. An average gain of 3 dB was exhibited between 5.5 and 6.5 GHz.

Gunn diodes have been used in conjunction with circulator-coupled networks in the design of high-level wideband transferred electron amplifiers that have a voltage gain-bandwidth product in excess of 10 dB for frequencies from 4 to about 16 GHz. Linear gains of 6 to 12 dB per stage and saturated-output-power levels in excess of 0.5 W have been realized [39]. Table 7-7-1 lists the performance of several amplifiers that have been designed since 1970.

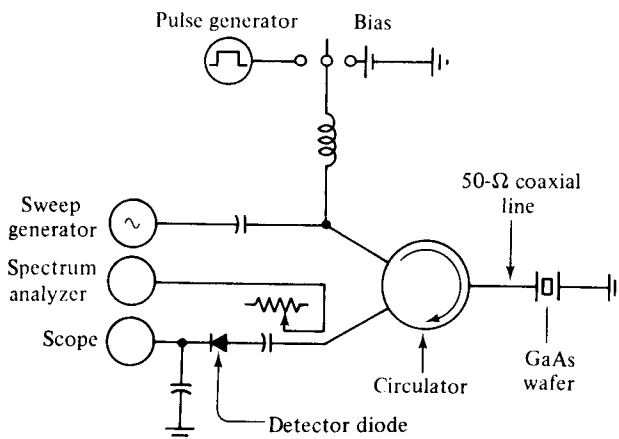


**Figure 7-7-3** Gunn-diode amplifier circuit. (After H. W. Thim [38]; reprinted by permission of IEEE, Inc.)

**TABLE 7-7-1** CW GUNN-DIODE AMPLIFIER PERFORMANCE

Frequency band	3-dB bandwidth (GHz)	Small signal gain (dB)	Power gain (dB)	Efficiency (%)
C	4.5–8.0	8	3	3
X	7.5–10.75	12	1.65	2.3
	8.0–12.0	6	1.8	2.5
Ku	12.0–16.0	6	1.5	2.5
	13.0–15.0	8	0.36	2

Source: After B.S. Perlman et al. [39]; reprinted by permission of IEEE, Inc.

## REFERENCES

- [1] SHOCKLEY, W., Negative resistance arising from transit time in semiconductor diodes. *Bell System Tech. J.*, **33**, 799–826, July 1954.
- [2] RIDLEY, B. K., and T. B. WATKINS, The possibility of negative resistance effects in semiconductors. *Proc. Phys. Soc.*, **78**, 293–304, August 1961.
- [3] HILSUM, C., Transferred electron amplifiers and oscillators. *Proc. IEEE*, **50**, 185–189, February 1962.
- [4] GUNN, J. B., Microwave oscillations of current in III-V semiconductors. *Solid-state Communications*, **1**, 89–91, September 1963.
- [5] RIDLEY, B. K., Specific negative resistance in solids. *Proc. Phys. Soc. (London)*, **82**, 954–966, December 1963.
- [6] KROEMER, H., Theory of the Gunn effect. *Proc. IEEE*, **52**, 1736 (1964).
- [7] GUNN, J. B., Microwave oscillations of current in III-V semiconductors. *Solid-state Communications*, **1**, 88–91 (1963).
- [8] GUNN, J. B., Instabilities of current in III-V semiconductors. *IBM J. Res. Develop.*, **8**, 141–159, April 1964.
- [9] GUNN, J. B., Instabilities of current and of potential distribution in GaAs and InP. *7th Int. Conf. on Physics of Semiconductor "Plasma Effects in Solids,"* 199–207, Tokyo, 1964.
- [10] KROEMER, H., Proposed negative-mass microwave amplifier. *Physical Rev.*, **109**, No. 5, 1856, March 1, 1958.
- [11] KROEMER, H., The physical principles of a negative-mass amplifier. *Proc. IRE*, **47**, 397–406, March 1959.
- [12] COPELAND, J. A., Bulk negative-resistance semiconductor devices. *IEEE Spectrum*, No. 5, 40, May 1967.
- [13] BUTCHER, P. N., and W. FAWCETT, Calculation of the velocity-field characteristics of gallium arsenide. *Appl. Phys. Letters*, **21**, 498 (1966).
- [14] CONWELL, E. M. and M. O. VASSELL, High-field distribution function in GaAs. *IEEE Trans. on Electron Devices*, **ED-13**, 22 (1966).
- [15] RUCH, J. G., and G. S. KINO, Measurement of the velocity-field characteristics of gallium arsenide. *Appl. Phys. Letters*, **10**, 50 (1967).
- [16] KROEMER, H., Negative conductance in semiconductors. *IEEE Spectrum*, **5**, No. 1, 47, January 1968.
- [17] COPELAND, J. A., Characterization of bulk negative-resistance diode behavior. *IEEE Trans. on Electron Devices*, **ED-14**, No. 9, 436–441, September 1967.
- [18] ELLIOTT, B. J., J. B. GUNN, and J. C. McGRODDY, Bulk negative differential conductivity and traveling domains in *n*-type germanium. *Appl. Phys. Letters*, **11**, 253 (1967).
- [19] COPELAND, J. A., Stable space-charge layers in two-valley semiconductors. *J. Appl. Phys.*, **37**, No. 9, 3602, August 1966.
- [20] GUNN, J. B., Effect of domain and circuit properties on oscillations in GaAs. *IBM J. Res. Develop.*, 310–320, July 1966.
- [21] HOBSON, G. S., Some properties of Gunn-effect oscillations in a biconical cavity. *IEEE Trans. on Electron Devices*, **ED-14**, No. 9, 526–531, September 1967.
- [22] THIM, H. W., Computer study of bulk GaAs devices with random one-dimensional doping fluctuations. *J. Appl. Phys.*, **39**, 3897 (1968).

- [23] THIM, H. W., and M. R. BARBER, Observation of multiple high-field domains in  $n$ -GaAs. *Proc. IEEE*, **56**, 110 (1968).
- [24] UENOHARA, M., Bulk gallium arsenide devices. Chapter 16 in H. A. Watson (Ed.), *Microwave Semiconductor Devices and Their Circuit Application*. McGraw-Hill Book Company, New York, 1969.
- [25] COPELAND, J. A., CW operation of LSA oscillator diodes—44 to 88 GHz. *Bell System Tech. J.*, **46**, 284–287, January 1967.
- [26] WILSON, W. E., Pulsed LSA and TRAPATT sources for microwave systems. *Microwave J.*, **14**, No. 8, August 1971, 87–90.
- [27] G. B. L., Three-level oscillator in indium phosphide. *Physics Today*, **23**, 19–20, December 1970.
- [28] COLLIVER, D., and B. PREW, Indium phosphide: Is it practical for solid state microwave sources? *Electronics*, 110–113, April 10, 1972.
- [29] TAYLOR, B. C., and D. J. COLLIVER, Indium phosphide microwave oscillators. *IEEE Trans. on Electron Devices*, **ED-18**, No. 10, 835–840, October 1971.
- [30] FOYT, A. G., and A. L. MCWHORTER, The Gunn effect in polar semiconductors. *IEEE Trans. on Electron Devices*, **ED-13**, 79–87, January 1966.
- [31] LUDWIG, G. W., R. E. HALSTED, and M. AVEN, Current saturation and instability in CdTe and ZnSe. *IEEE Trans. on Electron Devices*, **ED-13**, 671, August–September 1966.
- [32] LUDWIG, G. W., Gunn effect in CdTe. *IEEE Trans. on Electron Devices*, **ED-14**, No. 9, 547–551, September 1967.
- [33] BUTCHER, P. N., and W. FAWCETT, *Proc. Phys. Soc. (London)*, **86**, 1205 (1965).
- [34] OLIVER, M. R., and A. G. FOYT, The Gunn effect in  $n$ -CdTe. *IEEE Trans. on Electron Devices*, **ED-14**, No. 9, 617–618, September 1967.
- [35] HILSUM, C., New developments in transferred electron effects. *Proc. 3rd Conf. on High Frequency Generation and Amplification: Devices and Applications*. August 17–19, 1971, Cornell University.
- [36] HIESLMAIR, H., ET AL., State of the art of solid-state and tube transmitters. *Microwave J.*, **26**, No. 10, 46–48, October 1983.
- [37] HAKKI, B. W., GaAs post-threshold microwave amplifier, mixer, and oscillator. *Proc. IEEE (Letters)*, **54**, 299–300, February 1966.
- [38] THIM, H. W., Linear microwave amplification with Gunn oscillators. *IEEE Trans. on Electron Devices*, **ED-14**, No. 9, 520–526, September 1967.

## SUGGESTED READINGS

- EASTMAN, L. F., *Gallium Arsenide Microwave Bulk and Transit-Time Devices*. Artech House, Dedham, Mass., 1973.
- MILNES, A. G., *Semiconductor Devices and Integrated Electronics*. Van Nostrand Reinhold Company, New York, 1980.
- SOOHOO, R. F., *Microwave Electronics*. Addison-Wesley Publishing Company, Reading, Mass., 1971.
- SZE, S. M., *Physics of Semiconductor Devices*, 2nd ed. John Wiley & Sons, New York, 1981.

## PROBLEMS

### Transferred Electron Devices (TEDs)

- 7-1.
  - a. Spell out the following abbreviated terms: LSA, InP, and CdTe.
  - b. Describe in detail the principles of the following terms: Gunn effect, high-field domain theory, two-valley theory, and three-valley theory.
  - c. Discuss the differences between transferred electron devices and avalanche transit-time devices.
- 7-2. Describe the operating principles of tunnel diodes, Gunn diodes, and LSA diodes.
- 7-3. Derive Eq. (7-2-11).
- 7-4. Describe the modes of operation for Gunn diodes.
- 7-5. Describe the Ridley-Watkins-Hilsum theory.
- 7-6. The LSA oscillation mode is defined between  $2 \times 10^4$  and  $2 \times 10^5$  ratios of doping over frequency as shown in Fig. 7-3-1. Derive Eqs. (7-3-7) and (7-3-9).
- 7-7. For a transit-time domain mode, the domain velocity is equal to the carrier drift velocity and is about  $10^7$  cm/s. Determine the drift length of the diode at a frequency of 8 GHz.